Nat Hazards (2013) 69:2179–2196
DOI 10.1007/s11069-013-0800-1

ORIGINAL PAPER

Spatial response patterns of subtropical forests to a heavy ice storm: a case study in Poyang Lake Basin, southern China

Leilei Shi · Huimin Wang · Wenjiang Zhang · Quanqin Shao · Fengting Yang · Zeqing Ma · Yidong Wang

Received: 13 January 2012 / Accepted: 13 July 2013 / Published online: 23 July 2013

Abstract In early 2008, an unexpected ice storm hits southern China, severely affected the subtropical forest ecosystems. We used the moderate resolution imaging spectroradiometer products of Enhanced Vegetation Index (EVI) corroborated with information gathered from field investigations to analyze the spatial patterns of forest damage in Poyang Lake Basin. The results showed that forests on windward aspects and 400–1,000 m elevation zones are sensitive to ice storm. The spatial pattern of forest damage after the ice storm can be understood in light of topographical sheltering effect. Due to the mountains of the basin blocked the cold flow and wind, the damage on windward aspects showed more severity than other aspects, which was similar like previous studies in North America. The most severe canopy loss beyond 63 % (EVI loss 0.085) occurring on 400–800 m elevation zones. The secondary severe forest damage was on 800–1,500 m elevation zones with canopy loss 33 % (EVI loss 0.035), which unlike previous studies in North American that found damage was rapidly decreased at these elevations. This observation fits the ecological disturbances theory suggests that ice storms generating greater damage in forests which less frequently impacted by ice disturbance events. There appears to be a broader pattern of forest damage associated with ice storm in subtropical forests than in temperate

L. Shi · H. Wang (✉) · W. Zhang · Q. Shao · F. Yang · Z. Ma
Qianyanzhou Ecological Station, Key Laboratory of Ecosystem Network Observation and Modeling, Institute of Geographic Sciences and Natural Resources Research, Chinese Academy of Sciences, A11, Datun Road, Chaoyang District, Beijing 100101, China
e-mail: wanghm@igsnrr.ac.cn

L. Shi
Key Laboratory of Tropical Forest Ecology, Xishuanbanna Tropical Botanical Garden, Chinese Academy of Sciences, Mengla 666303, Yunnan, China

W. Zhang
State Key Laboratory of Hydraulics and Mountain River Engineering, Sichuan University, Chengdu, China

Y. Wang
Tianjin Key Laboratory of Water Resources and Environment, Tianjin Normal University, Tianjin, China

regions. This implies that the subtropical forests are more vulnerable than temperate forests to ice storm disturbance.

Keywords Ice storm · Spatial patterns of forest damage · Poyang Lake Basin · MODIS · EVI

1 Introduction

Ice storm affects the structure and function of a forest ecosystem greatly and may cause economic loss in managed forests (King et al. 2005; Nykänen et al. 1997). As consequences of climate change, ice storm events tend to increase in frequency and magnitude around the globe (IPCC 2007; Strasser 2008). During an ice storm in a forested landscape, glaze ice accumulates on trees and results in the loss of branches and twigs from the forest canopy, and even in uprooted and fallen trees (Michael et al. 2001). For instance, in February 1994, an unusually large and destructive ice storm hits the United States from northeastern Texas to Virginia, causing over 3 billion dollars worth of damage and significant losses of standing timber. Studies have suggested that ice storm disturbance is the important factor affecting species composition and some critical ecosystem patterns and processes such as nutrient cycling and forests microenvironment (Foster et al. 1998). Studies on the role of ice storm on ecosystem processes and patterns are indispensable for comprehensive understanding of the ecosystem structure, function, and dynamics (Nykänen et al. 1997).

Topography is considered to be an important factor influencing localized patterns of ice storm in forested regions (Foster et al. 1998; Pellikka et al. 2000; Rhoads et al. 2002; Rollins et al. 2002). Ice accumulation which is determined by weather conditions and influenced by location and topography (Nykänen et al. 1997) controlled the forest damage induced by ice storm. However, there are some apparently contradictory results about spatial patterns of forest damage caused by ice storm in different regions. For instance, the damage of an ice storm was mainly concentrated on windward slopes in northeast America in 1998 (Millward and Kraft 2004; Millward et al. 2010). In contrast, in Australia, ice damages are often observed to be worse in sheltered sites in mountainous regions (Cremer 1983). While in central Europe, it was reported that ice storm damage occurred on all slopes (Rottmann 1985a, b). Combined effect of altitude, terrain, and climate conditions may be contribute to the inconsistency of these results. The variety results reflect the uncertainty of spatial patterns of forest damage caused by ice storms in difference regions.

Forests cover approximately 20.36 % of the land area of China (SFA 2010). Approximately 10 % of forests are threatened by ice storm disturbances (Shen 2008). Especially in subtropical forests, one of the most damaging events is ice glaze caused by freezing precipitation (Zhou et al. 2011). This region is one of the main biodiversity hotpots in China (Liu et al. 2003). It is not only the home of most of the high vascular plant species but also host many animal species of China. Changes in the structure of these forest ecosystems have profound impacts on biodiversity. Currently, China imports 63.84 million cubic meter timber every year (SFA 2010). Due to economic development, the timber demand is still increasing. The subtropical forests comprise the productive wood production of China (SFA 2010). Meanwhile, increasing timber demand and the awareness of certified sustainable forestry raises the pressure to forest management. Unfortunately, this

Fig. 1 Severe damage in a slash pine forest in the southern of Poyang Lake Basin, February 24, 2008

region is exposed to ice storm disturbances. Actually, ice storms are common in southern China (Zhou et al. 2011) and in North America (Millward and Kraft 2004). However, much of our understanding of ice storm come from studies on the intense ice storm events occurred in temperate forest (Nykänen et al. 1997; Millward and Kraft 2004; Millward et al. 2010). Understanding how subtropical forest responds to ice storm is therefore crucial for sound management practices on these forest plantations.

Between January 11 and February 2,2008, up to 100 mm of freezing rain was deposited over approximately 10 million hectares in southern China (Shen 2008). This storm was the most spatially extensive recorded in recent 50 years in southern China. Several studies have examined the impact of ice storm disturbance on the subtropical forest in southern China (Pan et al. 2009; Shao et al. 2011; Xiao et al. 2008). The studies indicate that ice storms have damage the forest canopy severely in some plantations and have a major impact on the environments. However, most damage assessment of the ice storm-related conducted based on site visits (Pan et al. 2009; Shao et al. 2011; Xiao et al. 2008). It is unclear whether it is valid to extrapolate the results of these ground studies to the broader landscape scales relevant to forest management and sustainability. However, more objective and spatially explicit means of mapping ice storm damage were needed to help understand the effects of this storm and to provide a baseline from which forest recovery could be monitored.

Ideally, a study of the impacts of the ice storm on forest ecosystem should include information both before and after the disturbance event. Nevertheless, forest damage caused by ice storms is hard to predict both in space and in time, so collecting data prior to a specific event is difficult. Remote sensing has a potential role in damage mapping because it can provide spatially explicit vegetation reflectance change due to disturbance. In particular, archived imagery such as MODIS may enable pre- and post-storm change analysis. Additional environmental information from topography or meteorology data may be combined with remotely sensed imagery to model and map damage regionally.

The Poyang Lake Basin was chosen as our study site because it has serious attacked by the 2008 ice storm (Fig. 1), and it has varied forest types and a complex terrain. In this study, we analyzed the spatial variation in forest damage caused by the ice storm using satellite images and field investigation data and wish to understand the spatial pattern of ice

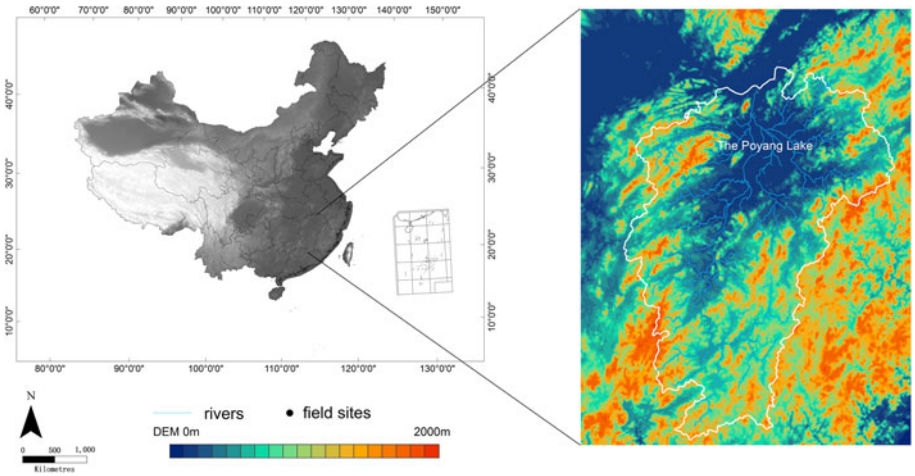

Fig. 2 Study area. The white lines indicate the boundary of Poyang Lake Basin, southeastern China. The 16.22×10^4 km^2 study area is bordered by Poyang Lake in the north and high peaks to the east, south, and west

storm disaster of subtropical forests. Our purpose focus on the following two questions: (1) how do topographical features (elevation, aspect, and slope) affect ice storm damage in the basin? and (2) what is the spatial pattern of ice damage of the subtropical forests in the basin?

2 Materials and methods

2.1 Study area

Poyang Lake Basin (113°34′36″–118°28′58″E, 24°29′14″–30°04′41″N) lies in southeastern China. It has a land area of 16.22×10^4 km^2 and forest coverage of 63.7 % (Zheng et al. 2009). Topography in this region is complex with an elevation range of 10–2,196 m above sea level. The west boundary is formed by Mufu Mountain, Lianyun Mountain, Jiuling Mountain, Wugong Mountain, and Luoxiao Mountain; the east boundary is formed by Jiuhua Mountain, Baihou Mountain, Huaiyu Mountain, and Wuyi Mountain, and the south boundary is formed by Nanling Mountain; with Ganjiang River cutting through from the south to north, forming Poyang Lake in the north (Fig. 2). The climate of the basin belongs to a moist middle subtropical monsoon type, and the landforms are characterized by red beds that are typical of the subtropical regions of China. The annual average temperature is 18.1 °C (Zhang et al. 2011). Annual precipitation is 1,400–1,800 mm. Subtropical forests cover this region by five main types: evergreen broad-leaved forest, mixed conifer and broad-leaved forest, coniferous forest, bamboo forest, and montane elfin forest (Fig. 3) (Xiao 2005). The original vegetation type of this region is subtropical evergreen broad-leaved forest. Because of a long history of over-felling has extremely destroyed the primary forests, artificial forestation and aerial seeding forestation since the 1970s dominated by coniferous species, such as masson pine (*Pinus massoniana* Lamb.), slash pine (*Pinus elliottii* Engelm.), and Chinese fir (*Cunninghamia lanceolata* (Lamb.) Hook.) (Shao et al. 2011).

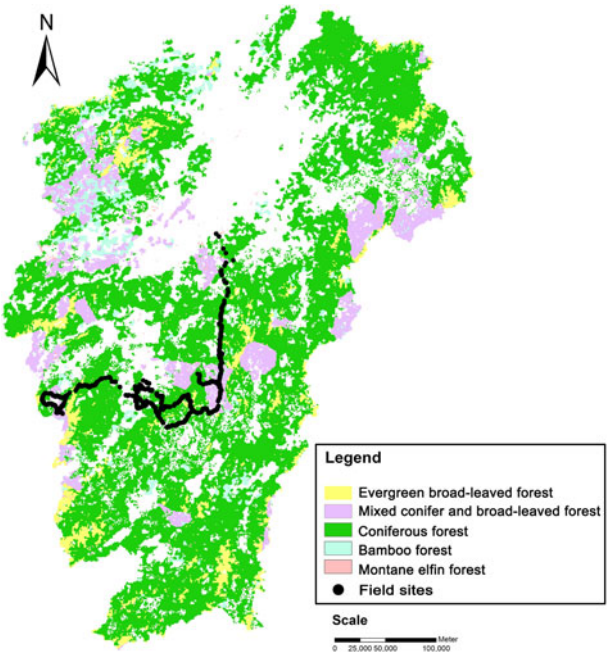

Fig. 3 The main five forest types of Poyang Lake Basin are generated from the 2007 forest inventory data (Zhang 2007). The *black dots* represent 100 field sites where forest damage was quantified after the 2008 ice storm. The *white area* represents areas without vegetation cover or undamaged

2.2 Data

2.2.1 Meteorological data

Meteorological data included daily average precipitation and wind speed during the 2008 ice storm (between January 11 and February 2, 2008), at eighteen China Central Meteorological Stations and fourteen local meteorological stations in Poyang Lake Basin. Spatial pattern of 23 days cumulative precipitation and average wind speed in the basin was simulated from values measured at the 32 meteorological stations by using the Regional Climate Model version 3 (RegCM3) (Fig. 4). Because of complex topography and large elevation range of the basin, we chosen RegCM3 which are much stronger and more realistic topographic forcing (Gao et al. 2012).

2.2.2 Satellite data

Moderate resolution imaging spectroradiometer (MODIS) land data products include the Normalized Difference Vegetation Index (NDVI) and the Enhanced Vegetation Index (EVI) (Justice et al. 2003). The MODIS 13Q1 Vegetation Indices were acquired from the Earth Observing System (EOS) data gateway of the NASA Land Processes Distributed Active Archive Center. One MODIS 13Q1 image is composite of 16-day images containing processed NDVI and EVI data at 250-m spatial resolution (Huete et al. 1999), fitting the spatial and temporal requirements for this study. A maximum of 64 observations are taken over the 16 days, and only the higher quality cloud-free filtered data are

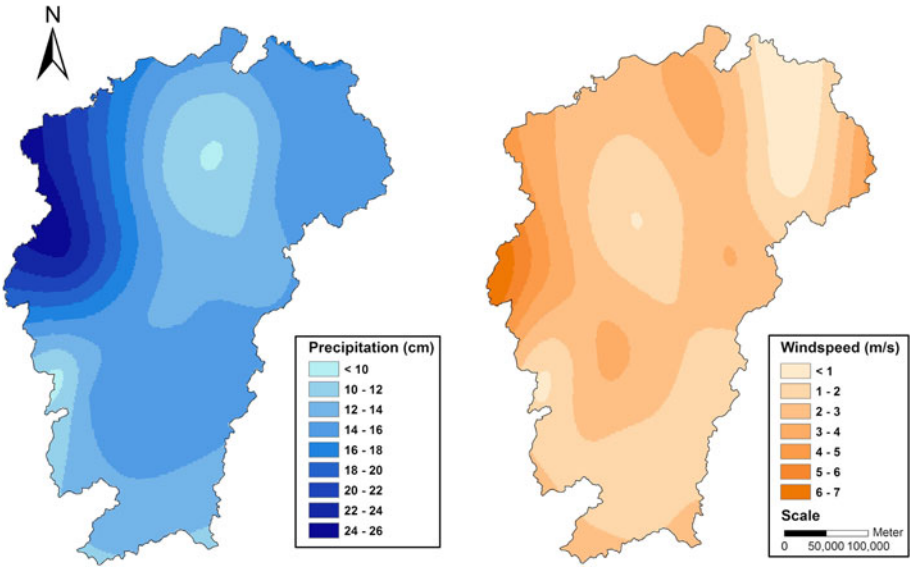

Fig. 4 Spatial pattern of cumulative precipitation and daily average wind speed in the Poyang Lake Basin between January 11 and February 2 2008 (simulated data from values measured at the 32 meteorological stations by using RegCM3)

combined to create a 16-day composite image (Huete et al. 2002). The MODIS VIs rely on the MODIS level-2 daily surface reflectance products which are atmospherically corrected (Vermote et al. 2002).

Both the NDVI and the EVI quantify the difference in reflectance in the visible red, where absorption in green leaves dominates, and the near-infrared (NIR) wavelengths, where light scattering by cell walls dominates (Tucker and Sellers 1986). However, compared to NDVI, the EVI offers improved sensitivity in high biomass regions and improved vegetation monitoring (Justice et al. 1998; Weier and Herring 2004). EVI also incorporates a soil adjustment factor as well as an atmosphere resistance term using the blue band in its formulation:

$$\mathrm{EVI} = G\frac{\rho_{\mathrm{NIR}} - \rho_{\mathrm{RED}}}{\rho_{\mathrm{NIR}} + (C_1 \times \rho_{\mathrm{RED}} - C_2 \times \rho_{\mathrm{BLUE}}) + L} \quad (1)$$

where ρ_{NIR} is the partially atmospherically corrected surface reflectance in the near-infrared (NIR) band (center wavelength = 858 nm, bandwidth = 841–876 nm), ρ_{RED} is the partially atmospherically corrected surface reflectance in the red band (center wavelength = 645 nm, bandwidth = 620–670 nm), ρ_{BLUE} is the partially atmospherically corrected surface reflectance in the blue band (center wavelength = 469 nm, bandwidth = 459–479 nm) (Anderson et al. 2005), L is the canopy background adjustment that addresses nonlinear, differential ρ_{NIR} and ρ_{RED} radiant transfer through the canopy, G is a gain factor, and C_1 and C_2 are the coefficients of the aerosol resistance term, which uses the blue band to correct for aerosol influences in the red band. The coefficients adopted in the EVI algorithm are as follows: $L = 1$, $C_1 = 6$, $C_2 = 7.5$ and $G = 2.5$ (Huete et al. 2002). We therefore chose to use the EVI in this study, as it may be a more appropriate product for use in disturbed subtropical forests, where soil background and vegetation baseline can be issues.

To guarantee the effect of the disturbance on vegetation reflectance, we selected one post-storm image taken on March 21, 2008, which was a 16-day composite image from March 21 to April 5. In our field observations, we found that over 20 days after the ice storm, the leaves of broken branches and trees were still green in subtropical forests. The irradiance of these green leaves on fallen branches brought interference for forest damage assessment. Until one and a half month after the ice storm, chlorophyll in the fallen leafs was began to fade out. And about 2 months after the ice storm, the color of fallen leafs mainly turned to yellow. On the other hand, over 2 months after the ice storm, shrubs and grasses were begin to recover owing to the spring season beginning in the early April. So, we selected the sixth MODIS 13Q1 image of 2008 which was a 16-day composite image taken from March 21 to April 5, which was between one and a half month and 2 months after the storm.

Besides, a pre-storm image that included undamaged forest information was indispensable. To make sure pre- and post-storm images had similarity forest phenological, we selected images that taken in the same time period of a year as post-storm image. Based on data quality information included in the MOD13Q1 product, compare to images taken in 2006 and 2007, we found images taken in 2004 and 2005 have higher quality. According to meteorological data at eighteen China Central Meteorological Stations in Poyang Lake Basin, the images in 2006 and 2007 may be disturbed by clouds or rains. Between March 21 and April 5, 2006, 13 days received rain and the daily mean rainfall was up to 36 mm. From March 21 to April 5, 2007, 14 days received rain and the daily mean rainfall was 28 mm. In 2005, the forest phonology was quite different to normal years in the study area because of low spring temperature according to our previous study (Zhang et al. 2011). In addition, the ratio of lowest quality image in 2005 was quite high when comparing with that in 2004. From 2004 to 2007, there was no large scale of forestation, forest harvesting, or large scale of disaster happened in the study area according to local forestry data. Therefore, we chose the MODIS 13Q1 image taken on March 21, 2004, which was composed from March 6 to 21, 2004, as the pre-storm data eventually.

2.2.3 *Field survey data*

Field investigations were carried out from February 28 to March 9 and March 27 to April 24, 2008, along transect of typical forest damage from which 100 damage sample plots (sample size was 400 m $\times$ 400 m) were collected (Fig. 3). The transect was located in central and southern Poyang Lake Basin, including Jinggangshan City, Taihe County, Xingguo County, and Ningdu County, with Luoxiao Mountain in the west, Jitai Basin and Yushan Mountain in the middle, and Wuyi Mountain in the east. The climate of the transect belonged to a moist middle subtropical monsoon type, and the landforms were varied from plain, hills to mountains. The 100 sample plots included almost typical subtropical forest types of Poyang Lake Basin. The forest types of Jinggangshan city were dominated by natural broad-leaved forest, Chinese fir (*Cunninghamia lanceolata*) and mao-bamboo (*Phyllostachys pubescens)*, including 7,000 ha of secondary virgin forests that represent an important fraction of the world's subtropical evergreen broad-leaved forest. The dominant forests of Taihe County, which was located in the hinterland of Jitai Basin, were masson pine (*Pinus massoniana* Lamb.), slash pine (*Pinus elliottii* Engelm.), and Chinese fir (*Cunninghamia lanceolata* (Lamb.) Hook.), and forest coverage was 51.6 %. The geomorphology of Xingguo County was primarily low mountains and hills. Forests dominated by masson pine, and forest coverage reached 72.2 %. Ningdu County

was a typical hilly and mountainous area. Primary forest types were masson pine and Chinese fir, and forest coverage was 71 % (Shao et al. 2011).

The survey recorded the information of locations, tree species, the number of damaged trees, and damage types. The supplementary information included soil types and stand structure. Tree damage was including dislodging (uprooting and overturn), stem breakage, crown and branch breakage (crown breakage, tip breakage, and branch breakage), bending, and mixed damage. The physical damage was divided into three classes: natural recovered damage (crown breakage, tip breakage and branch breakage), natural unrecovered damage (bending, stem breakage, uprooting and overturning), and mixed damage. Next, the damage ratio of each class and the total damage ratio for a sample plot were calculated.

The damage ratio for a certain damage class of a sample plot (D_{per}) was calculated as follows:

$$D_{\text{per}} = N_d/N_t \times 100\,\% \tag{2}$$

where D_{per} was the damage rate in a sample plot of a certain damage class; the N_{d} was a number of trees for a certain damage class in a sample plot; and N_t was the total number of trees in a sample plot. And the total damage ratio in a sample plot was the sum of all class damage ratios.

2.2.4 *Surface data*

Digital elevation models (DEMs) of the Poyang Lake Basin were extracted from the 90 m resolution DEM data set of China. This data set was provided by the Data Sharing Infrastructure of Earth System Sciences, Institute of Geographic Sciences and Natural Resources Research, Chinese Academy of Sciences. Slope and aspect variables were derived from the DEM data set using standard GIS software. Because the 90 × 90 m DEM was higher resolution than that of the MODIS satellite images (250 × 250 m), we re-sampled the data using cubic convolution to assign an elevation to each MODIS pixel (Keys 1981).

2.3 Analytical methods

2.3.1 *Image preprocessing*

Topographic effect is an important phenomenon in digital remote sensing images, especially in hill and mountain areas. First, the radiance distortion caused by the difference of ground slope, and sun altitude angle corrected by using the terrain-balanced model based on images characteristic and DEM data. Second, non-vegetated areas, water bodies, and towns were excluded from the analysis (using MOD12Q1 Land Cover information). Although cloud effect was minimized when using 16-day composite images, pixels with no valid information over the whole 16-day period (e.g., shadow) may have remained. Thus, a filtering process was applied based on the data quality information included as an additional band in the MOD13Q1 product. Only pixels containing acceptable information were finally considered (pixels classified as "higher quality" and "highest quality," and those that did not represent clouds, snow, or shadows) (Solano et al. 2010; Roy et al. 2002).

2.3.2 Detecting changes

To evaluate forest canopy change resulting from ice damage, we subtracted EVI values calculated for the 2004 image from the 2008 image. For purposes of this study, we assumed that the 2008 ice storm represented the only major disturbance during the 2000s that significantly influenced forest canopy integrity to any large extent within the Poyang Lake Basin. We reviewed logging records held by the State Administration of Forestry to confirm that only minor amounts of tree removal had occurred between the 2004 and 2008 satellite images. While some tree removal within the study area was associated with post-storm salvage efforts, the acquisition of our 2008 image predated these operations. MOD13Q1 products that have been atmospherically corrected permitted us to satisfy the assumption that a zero mean for stable EVI values in the difference image reflected no forest canopy change. Negative values in the resultant EVI difference image were hypothesized to be forest locations that experienced varying degrees of damage resulting from the ice storm.

A smoothing technique was applied to the dataset using a mode filter with a 5×5 kernel (Jensen 1996) to spatially bound the impacted storm area. This was necessary, so that a reasonable estimate of the storm perimeter could be ascertained from the fuzzy edge evidenced in the unfiltered data. Binary masks were generated based upon these boundaries, to isolate lightly and heavily-impacted regions within the study area. The filtered data were not used in subsequent analyses, only as a guide to partitioning the storm-impacted areas.

2.3.3 Field verification and calibration

In digital image processing, change threshold boundaries are often not known a priori and are commonly arrived at empirically (Ekstrand 1994; Jensen 1996). To distinguish "true" forest damage from natural processes affecting vegetative vigor and density, we compared EVI difference with canopy loss calculations based on field data. In situ forest damage at the field sites was quantified via a 400 m transect at each site. Each field observation of percentage canopy damage was associated with coordinates obtained from a Global Positioning System (GPS) to make sure the test pixels within the 400 m field grid. The EVI difference plotted in Fig. 3 is the mean difference for a 2×2 cell area, roughly equivalent to the area of the field site covered.

Except for five mao-bamboo and shrub field sites (circle points in Fig. 5), EVI declined at all ice-damaged sites (black points in Fig. 5). The value increased between 0.01 and 0.03 in the five sites. To confirm that an increase in EVI occurred in other bamboo and shrub sites within the MODIS EVI scene, we calculated the EVI difference for 5 additional sites outside the zone of major ice damage. We found that the EVI increased by >0.1 in all these locations as well. The increase may indicate that bamboo and shrub forests have superior recovery capability. On another hand, although bamboo bended down by the ice storm, most of them were still alive with their leaves still green, based on our field investigation.

We created a nonlinear model using 91 forest damage measurements, randomly selected from the pool of 100 available estimates. Validation in the model's ability to predict canopy damage was tested using nine field observations (previously unused). Comparing canopy loss to EVI difference revealed a strong relationship (Fig. 5) and confirmed the utility of EVI difference for characterizing ice damage.

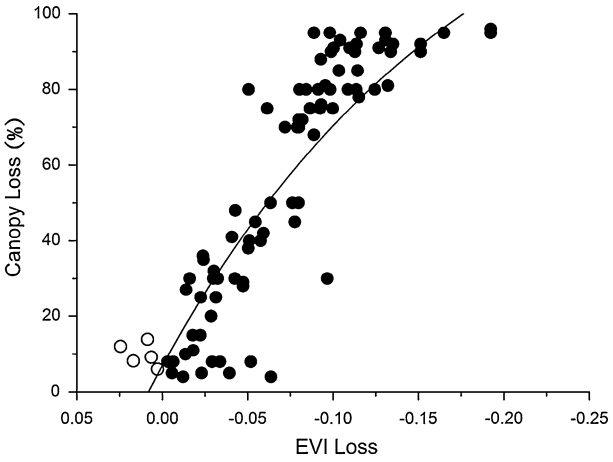

Fig. 5 Relationships between EVI difference and in situ estimates of ice storm damage. Canopy loss values were based on filed data and resulted from the Eq. 2. A negative value on the x axis indicates a decline in EVI between 2004 and 2008. The points in the panel represent the 91 sites where canopy loss was sampled after the 2008 ice storm. *Circle points* in the panel indicate the five bamboo and shrub sites. The regression *line* describes the relationship $y = -149.9 \times e^{x/0.181} + 156.82$, $R^2 = 0.69$, $p < 0.001$

2.3.4 Analysis of spatial patterns

Chi-square tests of correspondence and multiple regression analyses were used to analyze potential relationships of forest damage to topographic factors. For the Chi-square tests, we partitioned the EVI difference values into three classes containing equal numbers of pixels (cf. Millward and Kraft 2004; King et al. 2005). According to our field investigation, EVI values lost from −0.200 to −0.070, the tree damage types was were uprooting, overturn, and bending; EVI values lost from −0.070 to −0.008, the tree damage types present as stem breakage, crown breakage, tip breakage, and mixed damage; and EVI values change from −0.008 to 0.1, trees had slight damages, such as branch breakage. Hereafter, we referred to these categories of inferred ice damage as intense damage (−0.200 to −0.070), moderate damage (−0.070 to −0.008), and minor damage (−0.008 to 0.1). Pixels showing EVI difference <−0.2 or >0.1 were excluded because such changes were outside the observed range for the in situ data. The excluded pixels comprised only 2.3 % of all valid pixels.

Paired t test and one-way analysis of variance (ANOVA) followed by Bonferroni post hoc multiple comparisons were used to analyze potential relationships of forest damage to topographic factors. We created topographic categories from a digital elevation model (DEM) obtained from the resolution DEM data set of China. We performed a cubic convolution (Keys 1981) routine on the DEM (90 × 90 m pixels) of the study area to standardize it to a common spatial resolution with the EVI difference image (250 × 250 m pixels). Elevation, slope, and aspect were determined for each pixel in the DEM. Elevation was divided into 100 m zones. Aspect image was classified according to eight standard cardinal directions (N, NE, E, SE, S, SW, W, NW). Slope (0 to 65 degrees) was classified into seven categories in accordance with the geomorphological mapping rules of the International Geographical Union (IGU). We used a paired t test to examine the EVI and EVI difference of all used pixels between the two images from each year. We compared EVI and EVI change among aspects (in eight traditional classes), elevation, and slope,

using one-way analysis of variance (ANOVA) followed by Bonferroni post hoc multiple comparisons.

3 Results

3.1 Spatial variation in EVI loss affected by the 2008 ice storm

The mean EVI value of the study area was 0.28 ± 0.07 before the ice storm and was significantly decreased to 0.23 ± 0.05 after the ice storm (paired t test $p < 0.001$). The net decrease on EVI was 0.05 ± 0.005, which was corresponded to 40–46 % canopy lost according to the relationship between EVI loss and canopy loss (Fig. 5). The EVI loss affected by the ice storm was more extensive in the southern area, and the study area can be generally divided into southern and northern sections as shown in Fig. 6. The intense and moderate damages were most distributed in mountain areas of the basin. In northern section, the plain and hilly lands near the Poyang Lake were minor damaged by the ice storm. Meanwhile, the mountain areas on the west (Mufu Mountain, Lianyun Mountain, and Jiuling Mountain) of the Poyang Lake were more seriously damaged than those on the

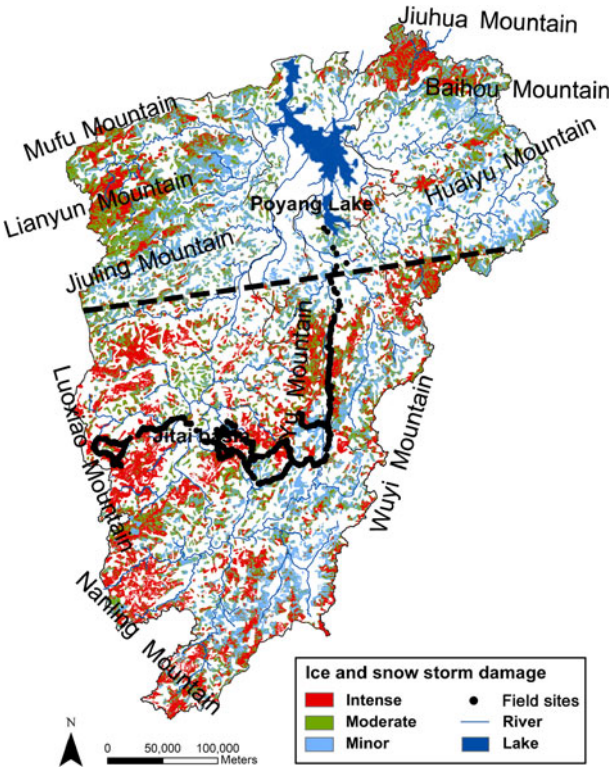

Fig. 6 Map of canopy damage within the study area forests resulting from the 2008 ice storm. *Red* and *green* areas represent major and moderately damaged forest, respectively. *White* areas are pixels excluded because these areas were not covered by forest. The heavy *dashed line* indicates the division between the northern and the southern sections. Streams and Poyang Lake are shown for geographical reference. For other landform characters, see Fig. 2

Table 1 Area of ice storm damaged forest within the more heavily damaged southern and lightly damaged northern portions of the study area, according to mean EVI change and damage classification

	Northern	Southern
Canopy loss (%)	27	48
Mean EVI loss	0.026	0.058
Standard error (SE)	0.0001	0.0001
Damage class		
Intense (km^2)	712,308 (21.3 %)	1,250,719 (37.4 %)
Moderate (km^2)	1,573,704 (43.8 %)	1,041,950 (29 %)

Table 2 Cramer's value and Chi-square values for damage with different topographic features

Topographic features	Cramer's value	Chi-square	*df*	*p*
Aspect	0.16	308.159	7	<0.001
Elevation	0.25	65,854.860	16	<0.001
Slope	0.30	45,510.180	6	<0.001

east (Jiuhua Mountian and Baihou Mountian). In southern section, damaged forests were concentrated on Luoxiao Mountain, Nanling Mountain, Yu Mountain, and Wuyi Mountain. The forest canopy loss in the southern section was about 48 %, which was approximately twice of that in the northern section of 27 %, and the ratio of the intensely damaged area in the southern section was 16.1 % higher than in the north (Table 1).

3.2 Spatial variation in EVI in relation to topographic features

Evaluation of the influence of topographic variables revealed that the three physical topographic features (aspect, elevation, and slope) were strongly correlated with ice storm damage. A Chi-square analysis of correspondence identified a significant relationship ($p < 0.001$) between topographic features and forest canopy damage via cross-tabulated method (Table 2). The result revealed that the Cramer's values for aspect, elevation, and slope were 0.16, 0.25, and 0.30, respectively, where Cramer's value ≥ 0.1 represents a minimum threshold for the presence of a relationship and value >0.3 denotes a strong correlation (Ott and Longnecker 2001). Though the three topographic features were correlated with the forest damage, the elevation and slope were more important than the aspect.

Figure 7 indicated that the EVI loss varied among different aspects (one-way ANOVA $p < 0.001$). EVI loss and intensely damaged area were the least on the southeast, south, and southwest-facing slopes and were the most on the north, northeast, east, west, and northwest-facing slopes. The difference of mean EVI loss among the later five aspects was tiny with the biggest gap of only 0.003 (canopy lost 9 %). The biggest difference of EVI loss among the eight aspects also small, which was 0.006 (canopy loss 12 %). The max EVI loss was 0.050 on the east aspect corresponding to forest canopy loss was 43 and 38 % of forest land were intensely damaged.

We also found a strong influence of elevation on the EVI loss and showed an inverse V-shape (Fig. 8a). The mean EVI loss increased rapidly with elevation under 600 m ASL and reached the peak on 600–700 m zone and decreased gradually between 700 and 1,600 m, while the EVI value increased when elevation exceeded 1,600 m. Further analysis showed that EVI loss under 1,600 m ASL was obviously caused by the ice storm using Bonferroni multiple comparison ($p < 0.05$). The largest EVI loss of the forest was

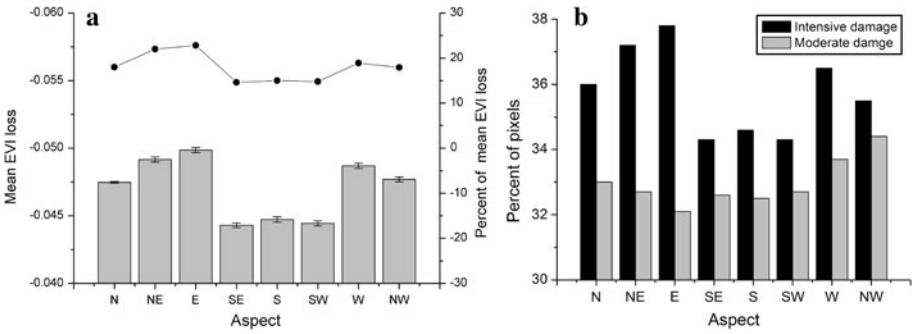

Fig. 7 Pattern of EVI loss (**a**) and the percent of damaged pixels (**b**) with respect to the influence of aspect. *Gray bars* and the *line* in **a** represent the value and percent of mean EVI change, after the 2008 ice storm on eight different aspects, respectively

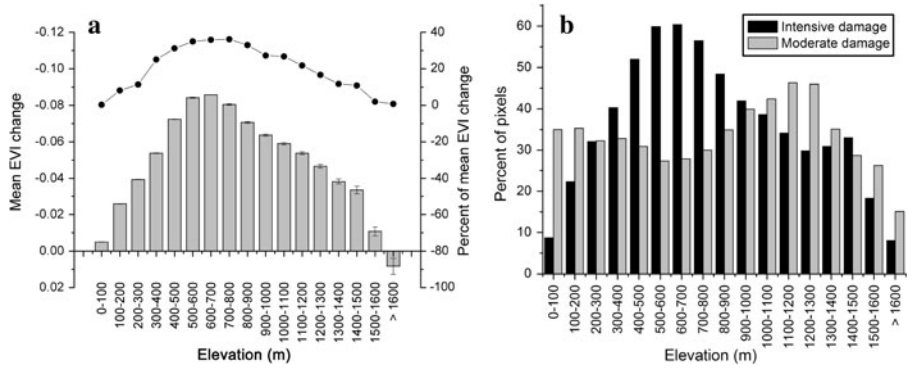

Fig. 8 Pattern of EVI loss (**a**) and the percent of damaged pixels (**b**) with respect to the influence of elevation. *Gray bars* and the *line* in **a** represent the value and percent of mean EVI change, after the 2008 ice storm on different elevation zones, respectively

concentrated on a belt between 400 and 800 m, with a EVI loss of, corresponding to forest canopy loss of 55–63 %. The EVI loss between 600 and 700 m was 0.085 and was approximately eight times that of the <100 m belt (EVI loss of 0.010).

The EVI loss increased as slope changed rapidly from gentle to moderate and then gradually declined with the increasing steepness (Fig. 9a). The highest EVI loss of 0.070, which was corresponding to a canopy loss of 55 %, occurred in a moderate slope with 15–35 degrees. When the slope steepness was more than 35 degrees, the mean EVI loss and the percentage of intensively damaged area gradually decreased. However, the percentage of moderately damaged area was almost equal in all categories when slope under 55 degrees (Fig. 9b).

4 Discussion

4.1 Topographical sheltering effect

The spatial pattern of EVI loss caused by the 2008 ice storm can be understood in light of interactions between atmosphere and topographical sheltering effects. Based on the

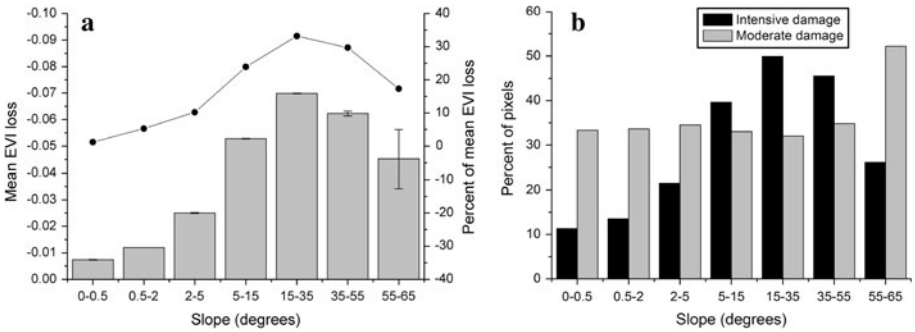

Fig. 9 Pattern of EVI loss (**a**) and the percent of damaged pixels (**b**) with respect to the influence of slope. *Gray bars* and the *line* in **a** represent the value and percent of mean EVI change, after the 2008 ice storm on different slopes, respectively

analysis of meteorological data, the intense and moderate damages were mainly distributed in areas with accumulation precipitation more than 140 mm and average wind speed beyond 2 m/s during the period of ice storm. There were two directions of cold flow and main wind during the ice storm: northeast and northwest (Zheng et al. 2008). Therefore, the mountains in the west and east probably blocked the heavy storm and intense winds, thereby protecting the south-facing slope areas when the ice storm came in from north. The topographical sheltering effect is also appeared in observations in northern American (Millward and Kraft 2004; Millward et al. 2010) and other natural disturbances in East Asia forest ecosystems, such as typhoon (Lee et al. 2008).

Aspect was an important topographic feature related to forest damage aroused by ice storm (Table 2). Many previous studies have shown that aspect was the most important terrain factor affecting temperate forest damage caused by ice storm in North American (Millward and Kraft 2004; Millward et al. 2010; Stueve et al. 2007) and north Europe (Solantie 1994; Solantie and Ahti 1980). On the windward slopes, wind will encourage substantial ice accumulate on branches and crown (Nykänen et al. 1997). On another hand, when the ice load is approach the maximum value which tree or its branches can support, a strong wind will inevitable aggravate the damage. The previous studies present that forests on the windward slopes are more affected by ice storm in North American (Millward and Kraft 2004; Millward et al. 2010). Our results showed similar phenomenon about aspect influence in southern China.

4.2 The broad pattern of subtropical forest damage to ice storm disturbance

There appears to be a broad pattern where subtropical forests that are impacted by ice storm than forests that are affected in temperate region. Our results revealed that the most intensive ice storm impact emerged in the middle elevations between 400 and 800 m in Poyang Lake Basin. But unlike the previous studies in North America found that damage decreased quickly at >800 m elevation zones (Millward and Kraft 2004), the intense impact of the ice storm reduced gradually at 800–1,500 m elevations (Fig. 8). Actually, EVI decrease was also serious at 800–1,500 m, where mean EVI loss exceeded 0.035 (canopy lost more than 33 %) (Fig. 8). The result corresponds to ecological disturbance theories. Compared to temperate forests, subtropical forests in Poyang Lake Basin were less impacted by ice storms according to local records. The adaptability hypothesis

suggests that forests that are impacted less frequently by ice storms have less resistant than forests that are more frequently affected by ice storm disturbance (Nykänen et al. 1997).

In addition, the upper limit of forest of this region was about 1,500 m (Zhang 2007). When above 1,500 m elevation, the vegetation type of these areas is high mountain meadow and alpine brushes, which have fine flexibility to ice storm (Nykänen et al. 1997). In addition, according to the local meteorological data, the daily average temperature of April, 2008, was about 0.5 °C higher than that of 2004. The higher temperature in early spring of 2008 might benefit for the meadow and brushes germinating. Consequently, there were no negative EVI changes above 1,600 m areas.

4.3 Influence of tree species and forest structure

Local evergreen broad-leaved forest in Poyang Lake Basin has the best resistance to ice storm disturbance. Tree species and forest structure have large influence on ice damage (Pellikka et al. 2000; Nykänen et al. 1997), because tree species and forest structure affect crown characteristics and wood strength, which are important components of tree stability when loaded with ice. In Europe, coniferous trees are generally more susceptible to ice storm than deciduous tree species (Nykänen et al. 1997). Based on our field investigation, we also found the similar phenomena in Poyang Lake Basin. Along the field site transect (Fig. 3), we found evergreen broad-leaved forest of on Luoxiao Mountain showed the lightest damage extent, and closed natural secondary mixed deciduous and broad-leaved forest was damaged severely due to high ice accumulation on intertwined shrubs. The most serious damage was found in coniferous forests, probably because its needle leave provides more beneficial interface for ice accumulation. For instance, slash pine showed a damage rate of 61.3 % of samples in Taihe county, of which 70.4 % cannot recover naturally. Masson pine was the native pioneer species, 52.5 % were damaged in Nanling Mountain, of which 60.9 % cannot recovery naturally. Chinese fir was a local tree species and samples showed a damage ratio of 46 %, in Taihe county and Yu Mountain. Because of the Poyang Lake Basin has a very large extent (16.22×10^4 km^2), and the forest types are varied and complex, therefore, we need to do more specific study to understand the relationship between forest types and forest damage aroused by ice storm in this region.

Overall, the results indicate that we should pay more attention to the windward aspect areas and 400–1,500 m elevation zones in subtropical forest management. These findings may be also region-specific, which are easy to find in places such as subtropical China but not in the temperate areas. The explanations in our study need to be further validated through more ground observations. Some theoretical or empirical ecological models may be used to study the ice storm in next step, while they will need to explicitly consider subtropical forests characteristics. For forest management and forest recovery, spatial scaling is an important issue and would require more work than conducted here.

5 Conclusion

The rapid decrease in forest greenness after the ice storm in subtropical China will help assessment the spatial pattern of forest damage. Our results present the spatial analysis of the magnitude and extent of ice damage across a large forested area in a subtropical region. We consider that similar patterns common occur when ice storms strike mountainous terrain in southern China. Remote sensing data can be used to construct the pre- and post-event spatial and temporal patterns of vegetation conditions in subtropical forests, which

can be applied to forest management or develop new hypotheses to guide-based studies. But satellite data cannot provide direct information about mechanisms controlling the impact dynamics of large extreme disturbances. To represent disturbance impact realistically, models may have to employ mechanisms to enable roles of life-history strategies of species in simulating post-disturbance vegetation dynamics. A close collaboration between the remote sensing, ground experimental, ecological theories, and large scale models is needed to advance the study of large extreme disturbance in subtropical forest ecosystems. Major findings from this study reflect the boarder spatial pattern of forest damage in the ice storm of subtropical forest than in North American. The results indicate that we should and pay attention to the windward aspect areas and 400–1,500 m elevation zones in forest management. In forest ecosystem, restoration and reconstruction need to consider about add more local evergreen broad-leaved species and abide the rule of matching tree species with site conditions as much as possible to guarantee the resistance of forest ecosystems to disaster.

Acknowledgments This research was supported by the "National Key Basic Research Program of China" (2012CB416903, 2009CB421101), the "Strategic Priority Research Program" of the Chinese Academy of Sciences,Climate Change: Carbon Budget and Relevant Issues (XDA05070302), the National Natural Science Foundation of China (31070559), the Knowledge Innovation Project of the Chinese Academy of Sciences (KZCX2-YW-Q1-14), and the Hundred Talents Program of the Chinese Academy of Sciences.

References

Anderson LO, Shimabukuro YE, Arai E (2005) Multitemporal fraction images derived from Terra MODIS data for analysing land cover change over the Amazon region. Int J Remote Sens 26:2251–2257

Cremer KW (1983) Snow damage in Eucalypt forests. Austral For 46:48–52

Ekstrand S (1994) Assessment of forest damage with Landsat TM: correction for varying forest stand characteristics. Remote Sens Environ 47:218–235

Foster DR, Knight DH, Franklin JF (1998) Landscape patterns and legacies resulting from large, infrequent forest disturbances. Ecosystems 1:497–510

Gao XJ, Shi Y, Zhang DF, Giorgi F (2012) Climate change in China in the 21st century as simulated by a high resolution regional climate model. Chin Sci Bull 10:1188–1195

Huete A, Justice C, Leewen W (1999) MODIS vegetation index (MOD13) algorithm theoretical basis document. Version 3. http://modis.gsfc.nasa.gov/data/atbd/atbd_mod13.pdf. Accessed 10 Jan 2012

Huete A, Didan K, Miura T, Rodiriguez EP, Gao X, Ferreira LG (2002) Overview of the radiometric and biophysical performance of the MODIS vegetation indices. Remote Sens Environ 83:195–213

IPCC (2007) IPCC fourth assessment report. Working group I: the physical science basis of climate change. http://ipcc-wg1ucaredu/wg1/wg1-reporthtml,last. Accessed 10 Jan 2012

Jensen JR (1996) Introductory digital image processing: a remote sensing perspective. Prentice Hall, Upper Saddle River, pp 230–257

Justice CO, Vermote E, Townshend JRG, Defries R, Roy DP, Hall DK, Salomonson VV, Privette JL, Riggs G, Strahler A, Lucht W, Myneni RB, Knyazikhin Y, Running SW, Nemani RR, Wan ZM, Huete AR, van Leeuwen W, Wolfe RE, Giglio L, Muller JP, Lewis P, Barnsley MJ (1998) The moderate resolution imaging spectroradiometer (MODIS): land remote sensing for global change research. Ieee T Geosci Remote 36:1228–1249

Justice CO, Smith R, Gill AM, Csiszar I (2003) A review of current space-based fire monitoring in Australia and the GOFC/GOLD program for international coordination. Int J Wildland Fire 12:247–258

Keys RG (1981) Cubic convolution interpolation for digital image-processing. IEEE Trans Acoust Speech 29:1153–1160

King DJ, Olthof I, Pellikka KE, Seed ED, Butson C (2005) Modelling and mapping damage to forests from an ice storm using remote sensing and environmental data. Nat Hazards 35:321–342

Lee MF, Lin TC, Vadeboncoeur M, Hwong JL (2008) Remote sensing assessment of forest damage in relation to 1996 strong typhoon Herb at Lienhuachi Experimental Forest. Taiwan. Forest Ecol Manag 225:3297–3306

Liu J, Ouyang Z, Pimm SL, Raven PH, Wang X, Miao H, Han N (2003) Protecting China's biodiversity. Science 300:1240–1242
Michael CH, Ken A, Martin JL (2001) Impact of a major ice storm on an old-growth hardwood forest. Can J Bot 79:70–75
Millward AA, Kraft CE (2004) Physical influences of landscape on a large-extent ecological disturbance: the northeastern North American ice storm of 1998. Landscape Ecol 19:99–111
Millward AA, Kraft CE, Warren DR (2010) Ice storm damage greater along the Terrestrial-Aquatic interface in forested landscapes. Ecosystems 13:249–260
Nykänen M-L, Peltola H, Quine C, Kellomäki S, Broadgate M (1997) Factors affecting snow damage of trees with particular reference to European conditions. Silva Fenn 31:193–213
Ott L, Longnecker M (2001) An introduction to statistical methods and data analysis. Duxbury, Pacific Grove, pp 138–158
Pan YY, Liu YQ, Wang YY (2009) Analyze the 2008 freezing rain disaster in southwest Zhejiang. Journal of Anhui Agri 37:1731–1733 (in Chinese with English abstract)
Pellikka P, Seed ED, King DJ (2000) Modelling deciduous forest ice storm damage using aerial CIR imagery and hemispheric photography. Can J Remote Sens 26:394–405
Rhoads AG, Hamburg SP, Fahey TJ, Siccama TG, Hane EN, Battles J, Cogbill C, Randall J, Wilson G (2002) Effects of an intense ice storm on the structure of a northern hardwood forest. Can J For Res 32:1763–1775
Rollins MG, Morgan P, Swetnam T (2002) Landscape-scale controls over 20th century fire occurrence in two large Rocky Mountain (USA) wilderness areas. Landscape Ecol 17:539–557
Rottmann M (1985a) Schneebruchschäden in nadelholzbeständen. Beiträge zur beurteilung der schneebruchgefährdung, zur schadensvorbeugung und zur behandlung schneegeschädigter nadelholzbestände. J.D. Sauerlander's Verlag, Frankfurt am Main 32:159–176
Rottmann M (1985b) Waldbauliche konsequenzen aus schneebruchkatastrophen schweizerische. Zeitschrift fur Forstwesen 136:167–184
Roy DP, Borak JS, Devadiga S, Wolfe RE, Zheng M, Descloitres J (2002) The MODIS land product quality assessment approach. Remote Sens Environ 83:62–76
Shao QQ, Huang L, Liu JY, Kuang WH, Li J (2011) Analysis of forest damage caused by the snow and ice chaos along a transect across southern China in spring 2008. J Geogr Sci 21:219–234
Shen GF (2008) Pay attention to the big rain and snow freeze disaster impact on forestry in China. Scientia Silvae Sinicae 33:1 (in Chinses)
Solano R, Didan K, Jacobson A, Huete A (2010) MODIS Vegetation Indices (MOD13) C5 User's Guide. Version 1.00. University of Arizona, Terrestrial Biophysics and Remote Sensing Lab. http://earthobservatory.nasa.gov/Library/MeasuringVegetation/measuring_vegetation_6.html. Accessed 10 Jan 2012
Solantie R (1994) Effect of weather and climatological background on snow damage of forests in southern Finland in November 1991. Sliva Fennica 28:203–211
Solantie R, Ahti K (1980) The influence of weather in the snow damages for forests of South-Finland in 1959. Sliva Fennica 14:342–353 (in Finnish)
State forestry administration, P.R. China (2010) The seventh national forest resources inventory. Science press, Beijing
Strasser U (2008) Snow loads in a changing climate: new risks? Nat Hazards Earth Syst Sci 11:587–595
Stueve KM, Lafon CW, EIsaacs RE (2007) Spatial patterns of ice storm disturbance on a forested landscape in the Appalachian. Aara 39(1):20–30
Tucker CJ, Sellers PJ (1986) Satellite remote sensing of primary productivity. Int J Remote Sens 7:1395–1416
Vermote EF, El Saleous NZ, Justice CO (2002) Atmospheric correction of MODIS data in the visible to middle infrared: first results. Remote Sens Environ 83:97–111
Weier J, Herring D (2004) Measuring vegetation (NDVI & EVI). http://earthobservatory.nasa.gov/Library/MeasuringVegetation/measuring_vegetation_4.html. Accessed 10 Jan 2012
Xiao XWB (2005) Altas of forest resources of China. Science Press, Beijing, pp 38 (in Chinese with English abstract)
Xiao FM, Chen HX, Jiang XM, Li WH, Peng XH, Zhang XJ (2008) Investigation on the damage of m oso bamboo caused by freezing rain and snow in Anfu, Jiangxi Province. Scientia Silvae Sinicae 44:32–35 (in Chinese with English abstract)
Zhang XS (2007) Vegetation of China. Geological Publishing House, Beijing, pp 136 (in Chinese with English abstract)

Zhang WJ, Wang HM, Yang FT, Yi YH, Wen XF, Sun XM, Yu GR, Wang YD, Ning JC (2011) Underestimated effects of low temperature during early growing season on carbon sequestration of a subtropical coniferous plantation. Biogeosciences 8:1667–1678

Zheng J, Xu AH, Xu B (2008) Contrastive analysis of the freezing rain and heavy snow processes in 2008. Meteo Disater Reduct Res 31:29–35 (in Chinese with English abstract)

Zheng JG, Wu Q, Liu X (2009) Climate and circulation characteristics of freezing rain in Jiangxi. Meteorology and Disaster Reduction Research 32:45–49

Zhou B, Gu L, Ding Y, Shao L, Wu Z, Yang X, Li C, Li Z, Wang X, Cao Y, Zeng B, Yu M, Wang M, Wang S, Sun H, Duan A, An Y, Wang X, Kong W (2011) The great 2008 Chinese ice storm: its socio-economic–ecological impact and sustainability lessons learned Bull. Am. Meteorol. Soc. 92:47–60